THE BULLETIN OF OKAYAMA UNIVERSITY OF SCIENCE No. 39 A pp. 97-105 (2003)

Maximum power point tracking without current sensor in photovoltaic power system which consists of parallel flyback type inverters

Nobuyuki KASA

Department of Electronics Engineering,
Faculty of Engineering,
Okayama University of Science,
Ridai-cho 1-1, Okayama 700-0005, Japan
(Received November 7, 2003)

This paper presents a current sensor-less flyback inverter controlled by MPPT for a photovoltaic (PV) small power system. Although the proposed system has such small output power as 300 Watts, a few sets of PV small power systems can be easily connected in parallel for the higher output power requirements. When a PV system is constructed by a lot of small power ones, the total system-cost will become a matter of concern. To overcome this difficult problem, this paper proposes that no expensive dc current sensor is used in the PV system and the PV current can be estimated from the PV voltage. This novel current sensor-less flyback inverter is applied to the PV system operated by MPPT, which shows the satisfactory MPPT-performance as well as the system with a dc current sensor. This paper also treats the design method and the operation of the unique flyback inverter with center-taped secondary winding. Finally, the parallel inverter system in which the outputs of the inverters connect each other is constructed, and the experimental results show that the parallel system gets larger power than the conventional one when the PV array is partially shaded by buildings.

1 Introduction

Photovoltaic (PV) systems have been developed to overcome an energy crisis in terms of ecology. The PV power conditioner in the PV system usually consists of both a dc-dc converter to control the PV voltage and a voltage source inverter to connect to the utility ac grid line. As a PV panel or a solar cell panel can generates rather small electric output power of approximately 100 Watts per one square meter at the fine weather condition, the maximum power point tracking (MPPT) technique is adopted to the PV power conditioner in order to utilize the PV array efficiently.

The PV voltage and PV current are required to calculate the PV output power for the MPPT operation. Therefore the expensive dc current sensor is absolutely required, which is the worrisome problem for the PV small power system. There are a lot of main circuit configurations for the PV power conditioners that are suitable for the ratings of less than 1k Watts as listed in the literature [1-10], Dr. Iida had proposed a kind of Buck-boost type inverter which has two sets of ac semiconductor switches to convert dc power to ac power [4]. However, this proposed inverter requires two sets of the dc sources of PV arrays, which supply the positive and negative half cycle current to utility ac gird line, respectively. This proposed inverter circuit has been improved to "one dc source type inverter" as reported in the literature [11-13]. One of the revised main circuit configurations is named the "flyback inverter with center-tapped secondary winding [13]".

In this paper, the "flyback inverter with center-tapped winding" is used to prove the operating performance of the newly proposed "current sensor-less flyback inverter". The "flyback inverter with center-tapped secondary winding" is already presented in the literature [12-14]; however, it is not so familiar that the features will be summarized as follows; No dc-dc converter is required, as the flyback inverter can directly convert the specified dc power to ac power, where the dc voltage is unrelated to the operation. The main circuit configuration becomes very simple and the number of the used power semiconductor switches is less than that of conventional one, which will contribute to the cost-reduction of the total system. As the electric potential of the PV array can be fixed to the ground potential, there happens no troublesome discharge current caused by the static capacity between the PV array and the ground, on the other hand, this discharge current becomes inevitable one, when the conventional bridge inverter circuit configuration is applied. The control algorithm is very simple and the open loop control method is enough for the PV power conditioner.

There are some problems in MPPT of the conventional PV system. When some pieces of PV panels are shaded by buildings or clouds, there appear some local maximum power points and the function may not track the true maximum point of power. The paper which treats the problems of series connected PV cells in a PV panel has been published in the literature[15-16]. In this paper, the parallel inverter system in which the outputs of inverters connect each other is proposed, and the parallel system may get larger power than the conventional one when the PV array is partially shaded by buildings.

The detail design-method of the flyback inverter is discussed at Section 2 in this paper. For the MPPT operation, the PV voltage and the PV current are required to calculate the PV output power. The PV current, averaged over half-cycle of the utility grid line, is calculated from the voltage across the capacitor connected to the PV array using a digital signal processor (DSP). Section 3 treats in detail the algorithm for the calculation including the flow chart. And the problems of MTTP are discussed, when the PV array is partially shaded by buildings. The experimental results show that the parallel system gets larger power than the conventional one when the PV array is partially shaded by buildings, and the details are shown in Section 4.

2 Center-tapped flyback inverter

2.1 Operation of secondary center-tapped flyback inverter

Fig. 1 shows a main circuit configuration of the prototyped PV power conditioner. The flyback inverter consists of three IGBTs, two diodes and a flyback transformer with center-tapped secondary winding. The flyback transformer has the functions not only to generate the ac power but also to isolate between the PV array and the utility ac grid line for the safety from some electric accident. The primary winding is connected to the PV array and IGBT1, and the gate pulse of which width is modulated by DSP drives the IGBT1. Two sets of ac semiconductor switches, which are composed of IGBT2 and diode D_1 in series and IGBT3 and D_2 in series, respectively, are connected to each terminal of secondary winding of the flyback transformer. They can switch reciprocally and synchronously with the polarity of the utility ac grid line. The switching sequence and waveforms are shown in Fig. 2.

Fig. 1 shows the operating modes of the flyback inverter with center-tapped secondary winding. The mode I is defined for the situation where IGBT1 is in on-state and all other IGBTs are in off-state and the stored energy in C_2 is discharged to the utility ac grid line, while the polarity of C_2 is synchronized with that

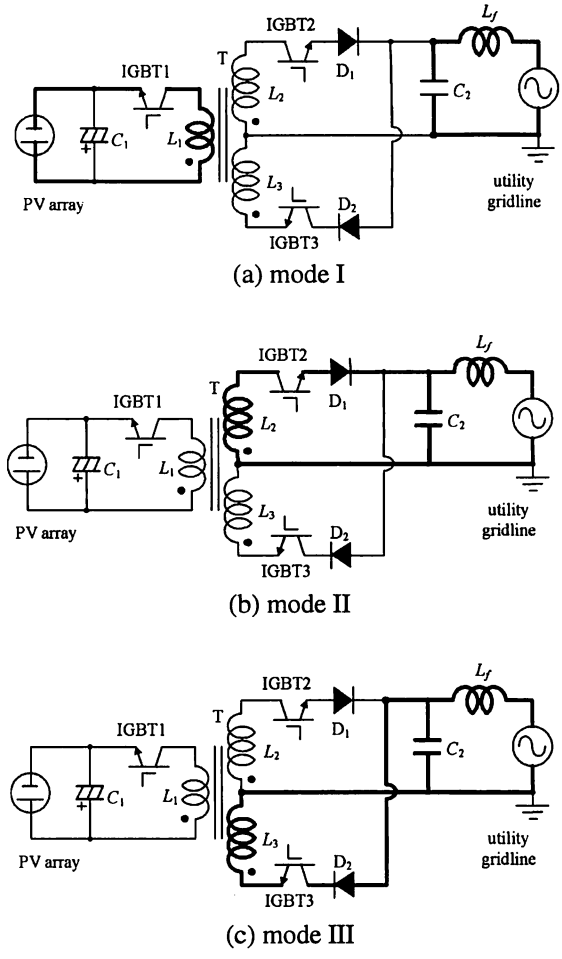

Figure 1: The circuit configuration and operation modes of flyback inverter with center-tapped secondary winding

of the utility ac grid line. The mode II is defined for the duration when IGBT2 is in on-state and all the rest are in off-state implying that the stored energies in T and C_2 are released to the utility ac grid line giving the positive polarity. The mode I and mode II are switched alternately at the high switching frequency during the positive half-cycle. The envelope of the peak current through the primary winding of the flyback transformer is so modulated as to be sinusoidal by the pulse-width modulation (PWM) gate pulse of IGBT1 and also is in phase to the utility ac gird line voltage. The mode III is for the negative half-cycle polarity. The mode I and mode III are switched alternately at the high switching frequency during the negative half-cycle. The current flown through IGBT1 is controlled just same as that described above excepting in the duration of the negative half-cycle of the utility ac grid line.

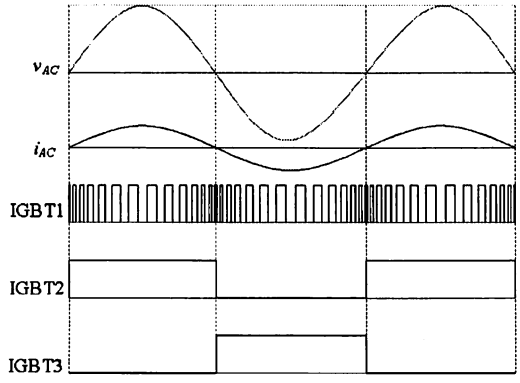

Figure 2: Switching sequence

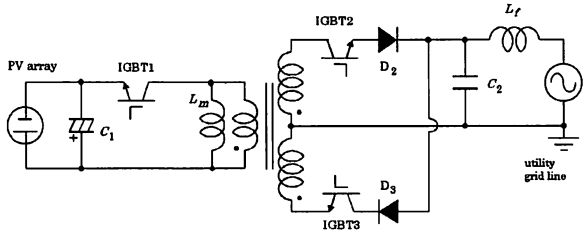

Figure 3: Circuit configuration applying the transformer model

2.2 Design of inductance

As the inductances of the windings of flyback transformer affect the performance of the inverter so strong that the careful design is required. In the following analysis, it is assumed that the transformer is the ideal one and has the equivalent magnetizing inductance of L_m in the primary side as shown in Fig. 3. As the turn ratio between the primary and the secondary winding of the flyback transformer is just two, the inductance between each terminal of secondary winding and center tap terminal becomes equal to L_m. Fig. 4 shows how the current in the magnetizing inductance of L_m excurses in the discontinuous current mode or DCM. The "I_P" is defined as the crest value of the enveloped peak current in L_m, when the inverter operates at the rated full power of P_{OUT} and the summation of t_{ON} and t_{OFF} is just equal to the duration of $1/(2Nf)$ at the crest current point, where, f is the utility grid line frequency and N is the total number of the switching periods during the half cycle $1/(2f)$. Using these letter symbols, the t_{ON} and t_{OFF} of IGBT1 can be expressed as

$$t_{ON} = \frac{L_m I_P}{v_C} \tag{1}$$

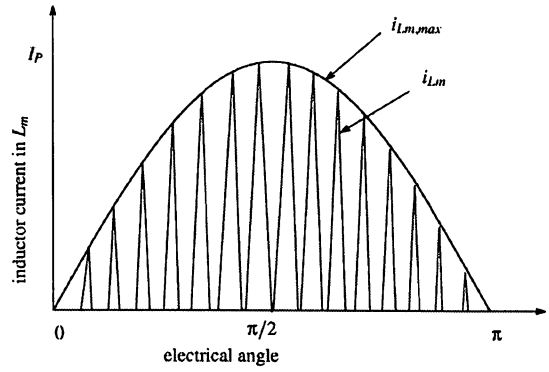

Figure 4: Inductor current mode at DCM

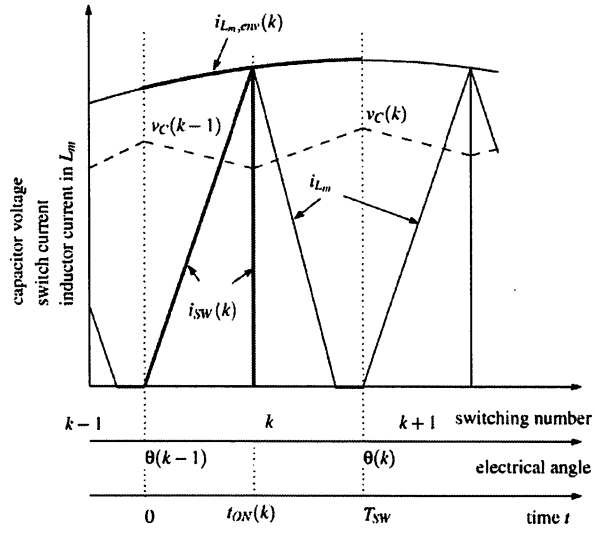

Figure 5: Waveforms of the switch current, the inductor current in L_m and the capacitor voltage during the k-th switching period

$$t_{OFF} = \frac{L_m I_P}{\sqrt{2}V_{AC}} \tag{2}$$

where, V_{AC} is the RMS value of utility grid line voltage and v_C is the capacitor voltage of C_1. Using eqns. 1 and 2, the L_m is expressed as

$$L_m = \frac{\sqrt{2}V_{AC}v_C}{2NfI_P(v_C + \sqrt{2}V_{AC})} \tag{3}$$

On the other hand, the rated maximum output power P_{OUT} is expressed as

$$P_{OUT} = fL_m I_P^2 \sum_{k=1}^{N} \sin^2\theta(k) \tag{4}$$

where, $\theta(k)$ is given by $k\pi/N$. By substituting eqn. 4 into eqn. 3, the inductance is finally given by

$$L_m = \frac{V_{AC}^2 v_C^2 \sum_{k=1}^{N} \sin^2\theta(k)}{2N^2 f(v_C + \sqrt{2}V_{AC})^2 P_{OUT}} \quad (5)$$

2.3 Calculation of switch-on duration

As shown in Fig. 5, the enveloped peak current in the magnetizing inductance of L_m during the arbitrary k-th switching period is expressed as

$$i_{L_m,env}(k) = I_P \sin\{\theta(k-1) + 2\pi ft\} \quad (6)$$

where, t is the time from the start point of the k-th switching period in second.

As $2\pi ft$ is small value, $i_{L_m,env}(k)$ is approximated as

$$i_{L_m,env}(k) \sim I_P\{\sin\theta(k-1) + 2\pi ft\cos\theta(k-1)\} \quad (7)$$

On the other hand, the switch current through the IGBT1 during the k-th switching period is expressed as

$$i_{SW}(k) = \frac{v_C - V_{th}}{R_1} + \left(-\frac{v_C - V_{th}}{R_1}\right) e^{-\frac{R_1}{L_m}t} \quad (8)$$

where, V_{th} is the threshold voltage of IGBT1, R_1 is the slope-on-resistance of IGBT1.

As t is small value, i_{SW}(k) can be approximated as

$$i_{SW}(k) \sim \frac{v_C - V_{th}}{L_m} t \quad (9)$$

When the intersection of i_{SW}(k) and $i_{L_m,env}(k)$ is set to the switch-on period, we obtain the pulse width $t_{ON}(k)$ of the k-th switching pulse by solving from eqns. 7 and 9 as

$$t_{ON}(k) = \frac{I_P \sin\theta(k-1)}{(v_C - V_{th})/L_m - 2\pi f I_P \cos\theta(k-1)} \quad (10)$$

3 Maximum power point tracking in parallel PV system

3.1 Maximum power point tracking without current sensor

As the PV array has the non-linear characteristics on the power versus voltage (PV) chart, the linear control theory cannot be applied to extract the maximum electric power from the PV array. The perturbation and observation method is often used for the maximum power point tracking (MPPT) in many PV systems. In this method, the operating points move toward the maximum power point by the periodically controlled

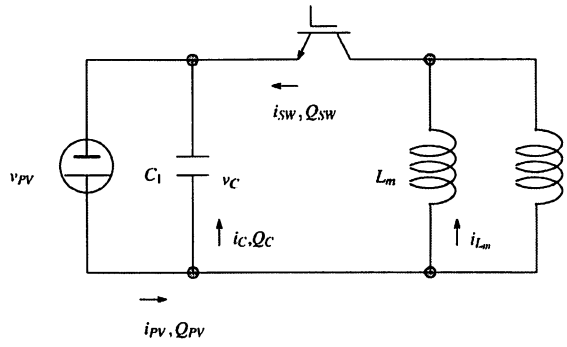

Figure 6: Equivalent circuit of flyback inverter (primary side only)

increase or decrease of the PV voltage. Usually, the maximum point is tracked by increasing or decreasing the duty ratio of on-state of the switching device. In the conventional system, it is required to calculate the PV output power, which is given by the product of the PV voltage and PV current. The PV current is usually detected by using the expensive dc current sensor and the alternative means to measure the dc current is desired for the cost-reduction. In this paper, it is proposed to calculate the PV current from the PV voltage as described below by the aid of digital signal processor (DSP) in the real time. It is paid attention that the PV current of i_{PV} consists of the summation of the capacitor current of i_C and the switch current of i_{SW} as shown Fig. 6.

$$i_{PV} = i_C + i_{SW} \quad (11)$$

When the eqn. 11 is integrated in the interval T_{SW} of a switching period, we get followings as

$$\int_0^{T_{SW}} i_{PV}\,dt = \int_0^{T_{SW}} i_C\,dt + \int_0^{T_{SW}} i_{SW}\,dt \quad (12)$$

The $\bar{i}_{PV}(k)$ is defined as the averaged current of $i_{PV}(k)$ in the interval T_{SW}, and the total amount of the electric charge which flows out from the PV array during the k-th switching period is defined as $Q_{PV}(k)$ and expressed as

$$\int_0^{T_{SW}} i_{PV}(k)\,dt \equiv Q_{PV}(k) = \bar{i}_{PV}(k) T_{SW} \quad (13)$$

In the same ways,

$$\int_0^{T_{SW}} i_C(k)\,dt \equiv Q_C(k) = \bar{i}_C(k) T_{SW} \quad (14)$$

$$\int_0^{T_{SW}} i_{SW}(k)dt \equiv Q_{SW}(k) = \bar{i}_{SW}(k)T_{SW} \quad (15)$$

Where, the $Q_C(k)$ and $Q_{SW}(k)$ are defined as the total amount of electric charges stored in the capacitor of C and flown through the switch of SW during interval T_{SW}, respectively. Fig. 6 shows the capacitor voltage and the switch current waveforms during the k-th switching period. When the $v_C(k-1)$ and $v_C(k)$ are defined as the capacitor voltages at the ends of the $(k-1)$-th and the k-th switching periods, respectively, the relation between these capacitor voltages and the electric charge of $Q_C(k)$ is expressed as

$$\int_0^{T_{SW}} i_C dt \equiv Q_C(k) \sim C\{v_C(k) - v_C(k-1)\} \quad (16)$$

The averaged capacitor current during the k-th switching period is given by

$$\bar{i}_C(k) = \frac{Q_C(k)}{T_{SW}} \sim f_{SW}C\{v_C(k) - v_C(k-1)\} \quad (17)$$

The average current of I_C is expressed as

$$I_C = \frac{1}{N}\sum_{k=1}^{N} \bar{i}_C(k) = 2fC\sum_{k=1}^{N}\{v_C(k) - v_C(k-1)\} \quad (18)$$

It can be is assumed that the switch current is composed by the magnetizing current in the flyback transformer. When the capacitor is so large that the fluctuation of the capacitor voltage during the switching period can be neglected, the switch current is expressed as

$$i_{SW}(k) \sim \frac{v_C(k)}{L_m}t \quad (19)$$

$$\text{where, } 0 \le t \le t_{ON}(k) \quad (20)$$

The relation between the electric charge and the switch current is expressed as

$$Q_{SW}(k) = \int_0^{T_{SW}} i_{SW}(k)dt \sim \frac{v_C(k)}{2L_m}t_{ON}^2(k) \quad (21)$$

From eqn. 15, the averaged switch current during the k-th switching period is expressed as

$$\bar{i}_{SW}(k) = \frac{Q_L(k)}{T_{SW}} \sim f_{SW}\frac{v_C(k)}{2L_m}t_{ON}^2(k) \quad (22)$$

The average switch current of I_{SW} is obtained as

$$I_{SW} = \frac{1}{N}\sum_{k=1}^{N}\bar{i}_{SW}(k) \sim \frac{f}{L_m}\sum_{k=1}^{N} v_C(k)t_{ON}^2(k) \quad (23)$$

Finally, the average PV current of I_{PV} can be estimated as

$$\begin{aligned} I_{PV} &= I_C + I_{SW} \\ &= 2fC\sum_{k=1}^{N}\{v_C(k) - v_C(k-1)\} \\ &+ \frac{f}{L_m}\sum_{k=1}^{N} v_C(k)t_{ON}^2(k) \end{aligned} \quad (24)$$

If the capacitor is so large that the fluctuation of the capacitor voltage during a switching period can be neglected, the PV current can be expressed as

$$I_{PV} = \frac{f}{L_m}\sum_{k=1}^{N} v_C(k)t_{ON}^2(k) \quad (25)$$

Fig. 7 shows a flowchart of the interrupt routine for the current estimation and MPPT. The differences between the conventional MPPT and the proposed one are the detection of the PV current and the controller of the duty ratio. To track the maximum power point, the PV output power is controlled by the duty ratio of the dc-dc converter in the conventional system. However, the duty ratio controls the waveform of the output current too and a pulse train in one cycle of the grid frequency is determined to keep the waveform of the output current sinusoidal in our proposed system. Therefore, the sampling rate of MPPT must be synchronized to the utility grid line frequency. To control the output power under these conditions, each duty ratio of the pulse train is calculated by multiplying a load factor to each duty ratio of the pulse train at the rated power. The sampling number k is used for the switching of IGBT1 and the sampling period is 104 μs in our experiment. On the other hand, the sampling number n is used for the MPPT operation and the sampling period is half cycle of the utility grid line. The process is as follows: At the beginning of it, the PV voltage is detected through the A/D converter. By using the detected voltage, $\bar{i}_C(k)$ and $\bar{i}_{SW}$ is calculated. When the switching number k is equal to N, the MPPT routine works. The arbitrary n-th of I_{PV} calculated by eqn. 24 is expressed as $I_{PV}(n)$. The n-th average PV voltage is averaged the voltage of $v_C(k)$ over the half-cycle of the utility grid line as

$$V_{PV}(n) = \frac{1}{N}\sum_{k=1}^{N} v_C(k) \quad (26)$$

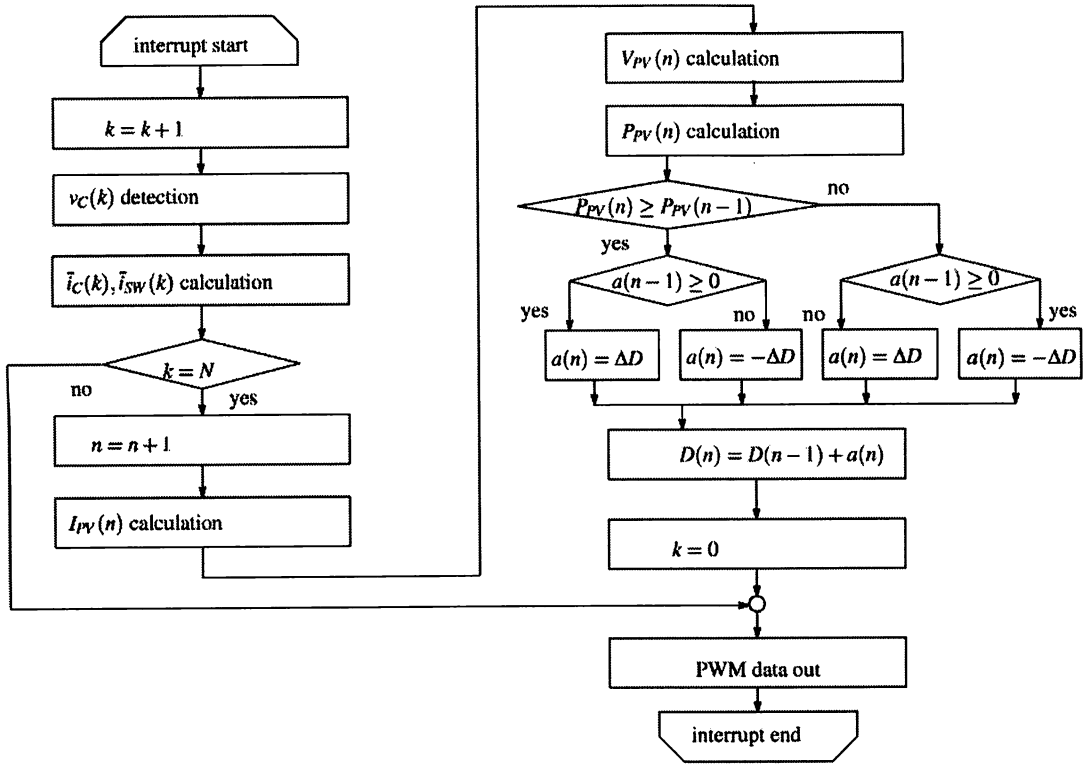

Figure 7: Flowchart of the interrupt routine for the current estimation and MPPT

The PV output power $P_{PV}(n)$ is delivered by multiplying the average PV voltage $V_{PV}(n)$ to the estimated PV current $I_{PV}(n)$. The processor DSP comparers the power $P_{PV}(n)$ to the $P_{PV}(n-1)$ that were calculated at the previous sampling. To get larger power than that at previous sampling, the load factor $D(n)$ is determined to increase or decrease ΔD, which is expressed as $a(n)$, based on the one at the previous sampling $a(n-1)$. The load factor $D(n)$ is expressed as

$$D(n) = D(n-1) + a(n). \tag{27}$$

In order not to distort the sinusoidal output waveform of the inverter, the sampling period coincides with the cycle of the grid frequency. Eqn.10 gives the pulse width of an arbitrary main switching pulse at the full load condition. However, to control the output power, each $t_{ON}(k)$ is multiplied by the load factor $D(n)$ on every half-cycle of the utility grid line.

3.2 Maximum power point tracking influenced by shade

Fig. 8 shows two sets of PV array, where each set of PV array consists of three PV panels connected in series and each panel has the maximum output power rating of 109W. In Fig. 8, one of the panels of PV2 is shaded by buildings. To investigate the partially shaded characteristics of PV array, the power versus voltage (P/V) characteristics of PV1 and PV2 are measured as shown in Fig. 9. It can be seen that the output power of PV2 is lower than that of PV1, as PV2 is partially shaded. PV1 has the maximum power point of 200 W (peak C) and on the other hand, PV2 has only 120 W (peak D). When PV1 and PV2 are connected in parallel, it can be seen that the total maximum output power becomes not 320W but 250 W showing two peaks A and B on the P/V curve as seen in Fig. 9. As the conventional operation of perturbation and observation method will start from the open voltage or high voltage of PV array, MPPT can only detect the first peak point B or local maximum point on the P/V characteristic curve. It means that the PV system can only deliver the output dc power of 200 W.

If each PV array has an inverter which is equipped an individual function of MPPT, the power 320W can be obtained. To equip the individual function of MPPT, the system has to have plural dc-dc converters or plural inverters. As these systems are used in parallel, the cost and the reliability are strongly demanded. Therefore, the proposed current sensor-less flyback inverter is suitable for these usages.

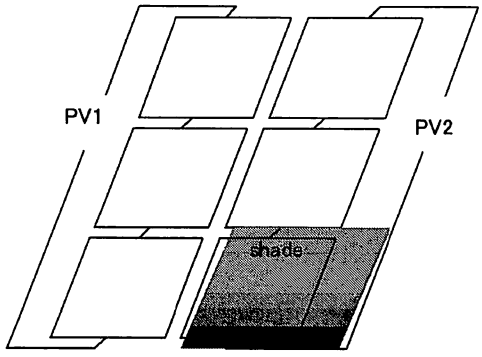

Figure 8: Two sets of photovoltaic arrays

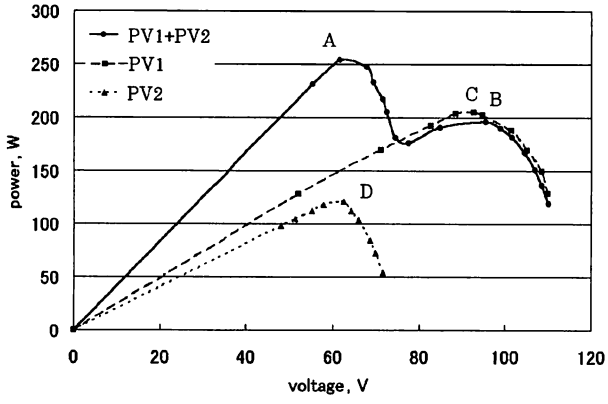

Figure 9: P-V characteristics

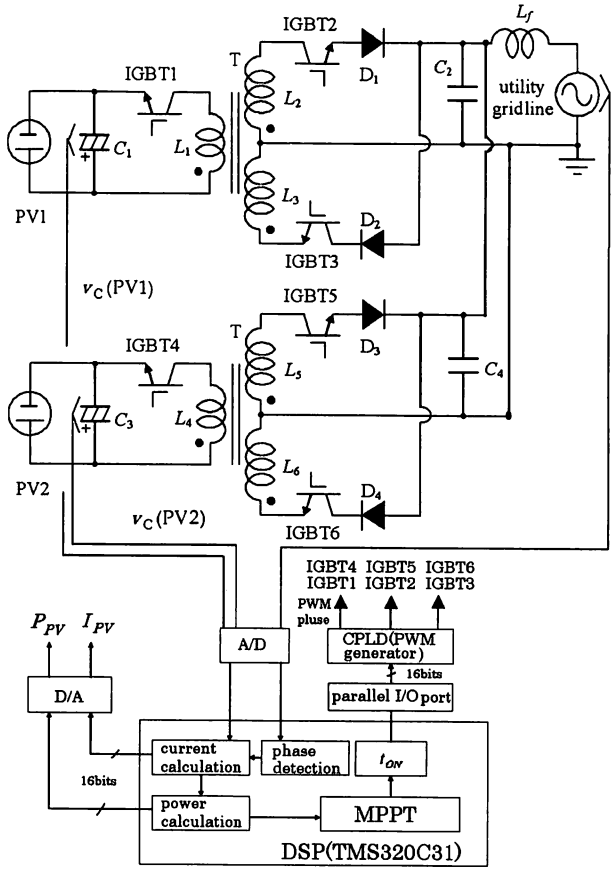

Figure 10: System configuration

4 Experimental Results

Fig. 10 shows our experimental system configuration. Three photovoltaic arrays are used as the input source of each inverter and the rated power of each PV array is 327W. The TI TMS320C31 DSP is used to calculate the PV current, track the maximum power point, control the whole power system and calculate each pulse width of IGBT. The data of pulse width is outputted through the digital output port and the data is encoded to the pulse width by digital circuits on a programmable logic device (CPLD). In this experimental system, the voltage and the current of the PV array are detected for the calculation and the monitoring. The switching frequency of the IGBT1 (9.6 kHz) is synchronized to the frequency of the utility grid line (60 Hz). The inductor current operates in DCM. The circuit parameters are listed in Table 1.

Fig. 11 shows the output voltage, the output current and the inductor current waveforms of the proposed inverter, with the output power of the inverter being 300 W. In Fig. 11a, the waveforms are the simulation results which are obtained from PSPICE. In Fig. 11b, the waveforms are experimental results by the prototype photovoltaic power system. Experimental results are in good agreement with simulation results. It is found that the proposed inverter supplies the AC power to the utility grid line with the power factor of nearly unity.

In order to verify the equations which estimate the PV current, the PV current which is calculated by the DSP is compared to the PV current which is measured by a dc current sensor tentatively connected between the PV array and the capacitor C_1. The calculated current data are delivered through the D/A converter that is installed on the DSP board as shown in Fig.10. In Fig.12, the upper waveform is the measured PV current

Table 1: Circuit parameters

L_1, L_2, L_3	$300\,\mu$H	C_1, C_3	$4700\,\mu$F
L_4, L_5, L_6	$300\,\mu$H	C_2, C_4	$12\,\mu$F
f	60Hz	V_{AC}	100V
N	80	f_{sw}	9.6kHz

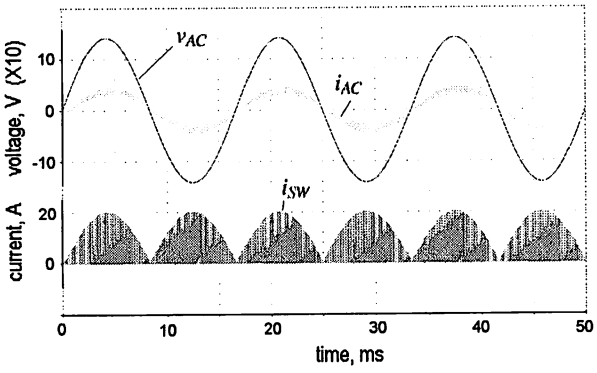

(a) simulation results

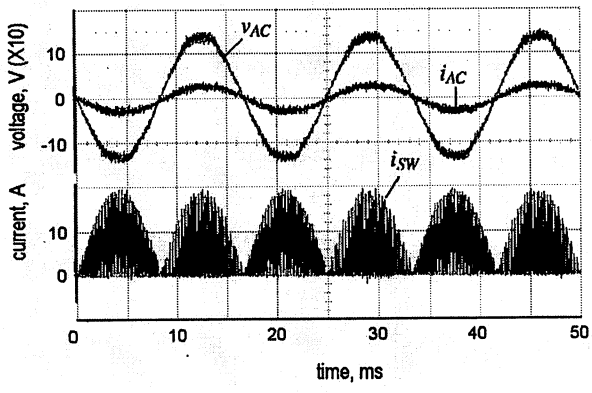

(b) experimental results

Figure 11: Output voltage and current, and inductor current waveforms

$I_{PV,CS}$ by the dc current sensor, on the other hand, the lower one is the one that is calculated by eqn.24. On the initial condition, the capacitor C_1 is not charged. When the system is switched on, the current which charges to the capacitor C_1 rises on the transient condition. In this figure, it is clear the both curves are similar to each other. It is found that there is a little bit of the delay on the lower waveform caused by the sampling period of the processor program.

Fig. 13 shows the experimental results of MPPT, when the PV2 is partially shaded as shown in Fig. 8. The upper waveform indicates the behavior of MPPT by the parallel inverters which have the function of the individual MPPT. As each inverter system can track the maximum power points C and D as shown in Fig. 9, the total power became about 315W. On the other hand, the conventional system tracks the local maximum power point B as shown in Fig. 9, and then the obtained power is only 200W as shown in the lower waveform in Fig. 13.

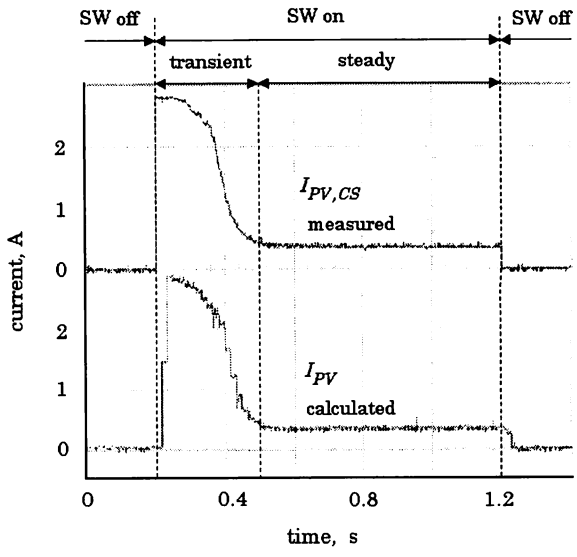

Figure 12: Waveforms of PV current

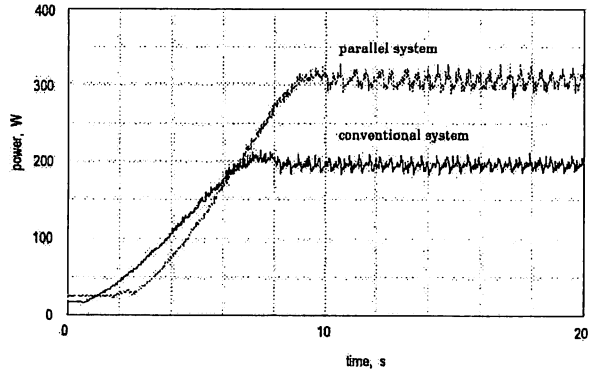

Figure 13: Behaviour of MPPT by parallel inverters

5 Conclusions

I have proposed a current sensor-less MPPT controlled flyback inverter for small scale PV systems. The used main circuit is the flyback inverter with the secondary center-tapped winding. The features of this circuit are the simplicity comparing to conventional one and its controller is implemented by DSP. Because the proposed system was able to control the output power with the open loop, it can calculate the PV power with detecting only the PV voltage. Therefore the maximum power point of the PV array can be obtained in the PV system without a current sensor as well as with a current sensor. I have constructed the parallel inverter system in which the outputs of inverters connect each other, and the parallel system can get larger power than the conventional one when the PV array is partially shaded by buildings.

6 Acknowledgement

The author would like to thank Prof. Takahiko Iida of Okayama University of Science, Japan for his idea of this main circuit topology and Mr. Ryotaro Yamada of Shindengen Electric Manufacturing CO., LTD, Japan for his help to this study.

7 References

1 NAGAO, M., HORIKAWA, H., and HARADA, K.: 'Photovoltaic system using buck-boost PWM inverter', *Trans. of IEEJ*, 1994, 114–D, pp.885-892

2 SAHA, S., SUNDARSINGH, V.P.: 'Novel grid-connected photovoltaic inverter', *IEE Proceedings –Gener. Transm. Distrib.* , 1996, 143 (2), pp.497-502

3 NAGAO, M., and HARADA, K.: 'Power flow of photovoltaic system using buck-boost PWM power inverters', *PEDS'96*, May, 1996, pp.114-149

4 MATSUI, S., IIDA, T.: 'A research and development of SMR-type inverter', Joint Conference of Cyugoku Chapters of Electrical Societies 1997, p.129, Oct. 1997 (in Japanese)

5 KASA, N., and IIDA, T.: 'A transformer-less single phase inverter using a buck-boost type chopper circuit for photovoltaic power system', *ICPE'98*, Oct. 1998, Seoul, Korea, pp. 978-981

6 KASA, N., IIDA, T., and IWAMOTO, H.: 'An inverter using buck-boost type chopper circuits for popular small-scale photovoltaic power system', *IEEE IECON'99*, Nov. 1999, Sanjose, US

7 KASA, N., IIDA, T., and IWAMOTO, H.: 'Maximum power point tracking with capacitor identifier for photovoltaic power system', *IEE Proceedings – Electric Power Application*, 2000, 147 (6), pp.497-502

8 SHIMIZU, T., NAKAMURA, N., and WADA, K.: 'A novel flyback-type utility interactive inverter for AC module systems', *ICPE'01*, Oct. 2001, Seoul, Korea, pp.518-522

9 KASA, N., IIDA, T., and MAJUMDAR, G.: 'Maximum power point tracking without current sensor for small scale photovoltaic power system', *ICPE'01*, Oct. 2001, Seoul, Korea, pp.631-634

10 KONISHI, Y., CHANDHAKET, S., OGURA, K., and NAKAOKA, M: 'Utility-interactive modulated sinewave inverter with a high frequency flyback transformer link for small-scale solar photovoltaic generator', *ICPE'01*, Oct. 2001, Seoul, Korea, pp.683-686

11 YAMADA, R., KASA, N., IIDA, T.: 'Photovoltaic systems with flyback type inverter', Joint Conference of Cyugoku Chapters of Electrical Societies 2001, No. 150507, 20th Oct. 2001 (in Japanese)

12 KASA, N., IIDA, T.: 'A flyback type inverter for small scale wind power generation system', Technical reports of Semiconductor Power Converter, SPC-02-16, 2nd Feb. 2002 (in Japanese)

13 KASA, N., IIDA, T.: 'Photovoltaic systems with flyback type inverter', Japan Society of Power Electronics, vol.27, pp.187-192, March 2002 (in Japanese)

14 SHIMIZU, T., WADA, K., NAKAMURA N.: 'A flyback-type single phase utility interactive inverter with low-frequency ripple current regulation on the DC input for an AC photovoltaic module system', PESC 2002, 23-27 June, 2002, Vol.3, pp.1483-1488

15 SHIMIZU, T., HIRIKATA, M. KAMEZAWA, T., WATANABE, H.: 'Generation control circuit for photovoltaic modules', *Trans. of IEEE on Power Elec.*, 2001, 16(3), pp.293-300

16 NISHIMURA, K., and EGUCHI, M.: 'String power conditioner for photovoltaic system with the function of multi-string MPPT', *Japan Society for Power Electronics*, 2002, 28(8)